Analysis of the spatial and temporal distribution of the 2001 earthquakes in El Salvador

B. Benito

Escuela Universitaria de Ingeniería Topográfica, Universidad Politécnica de Madrid, Campus Sur, Autovía de Valencia km 7, E28031 Madrid, Spain

J.M. Cepeda

Universidad Centroamericana Simeón Cañas, Boulevard Los Procéres, San Salvador, El Salvador

J.J. Martinez Diaz

Departamento de Geodinámica, Universidad Complutense, Madrid, Spain

ABSTRACT

This paper presents a study of the spatial and temporal distribution of the large destructive earthquakes that occurred in El Salvador during January and February 2001, together with the static stress transfer after each main shock, associated with their respective rupture processes. The sequence began with the magnitude M_W 7.7 earthquake of 13 January, located off the western Pacific Coast in the subduction zone between the Cocos and Caribbean plates. One month later, a second destructive earthquake of M_W 6.6 occurred in the Caribbean plate farther inland, the epicenter of which was located near San Pedro Nonualco. This shock was linked to the local faults beneath the volcanic arc and also produced significant damage. The two main shocks and their aftershock sequences, together with other minor events that followed successively, produced unusually intense activity in the zone, in a short interval of time. The aims of this study are to document the spatial and temporal evolution of each seismic sequence and also to understand the possible interaction between the different events. We have inferred that some events with M > 5 triggered other shocks with the same or different origin (subduction zone or local crustal faults). The Coulomb stress transfer has been studied, and some models developed, using the rupture parameters derived from the geometric distribution of aftershocks. These results suggest the existence of a dynamic interaction, since the 13 February event occurred in a zone where the Coulomb stress increased following the January 13 event. Subsequently, some further events with magnitude around M_W 5 in turn were located in other zones of increased stress associated with the two previous large earthquakes.

Keywords: seismicity of Central America, subduction, aftershock distributions, Coulomb stress transfer, triggering mechanism.

INTRODUCTION

On January 13, 2001, a destructive earthquake of M_W 7.7 (U.S. Geological Survey) struck El Salvador, Central America. The earthquake was centered at 12.80° N, 88.79° W with a focal depth of 40 km, in the subduction zone between the Cocos and Caribbean plates. This earthquake was followed by numerous aftershocks with the same origin; ~540 events with M > 2 occurred in the first month, and 4000 in the first six months, nearly half of which were larger than M 3.0.

Just one month later, on 13 February, a second major earthquake of M_W 6.6 occurred, this time located farther inland

*ma_ben@euitto.upm.es

B. Benito, J.M. Cepeda, and J.J. Martinez Diaz

(13.64° N, 88.94° W) and with a shallower focal depth of ~15 km. This earthquake, located near San Pedro Nonualco (30 km from San Salvador), was associated with the local fault system aligned with the Central American volcanic arc that bisects El Salvador from east to west. This shock was preceded by numerous local events, ~100 events between 13 January and 13 February (M > 2), and followed by numerous aftershocks, 685 during the first month and 1300 in the first six months.

A third moderate-magnitude event (m_b = 5.1, CIG) occurred four days later, on 17 February, located south of metropolitan San Salvador (12.90° N, 89.10° W), but also associated with faulting along the volcanic axis.

The seismicity map with the epicenters of the events of 2001 in El Salvador and surrounding areas, recorded by the Center for Geotechnical Investigations (CIG), is shown in Figure 1.

Besides the three principal earthquakes described above, other events with magnitude close to and larger than M 5 followed the first shock until September 2001, alternating between events of the subduction zone and those of the volcanic arc.
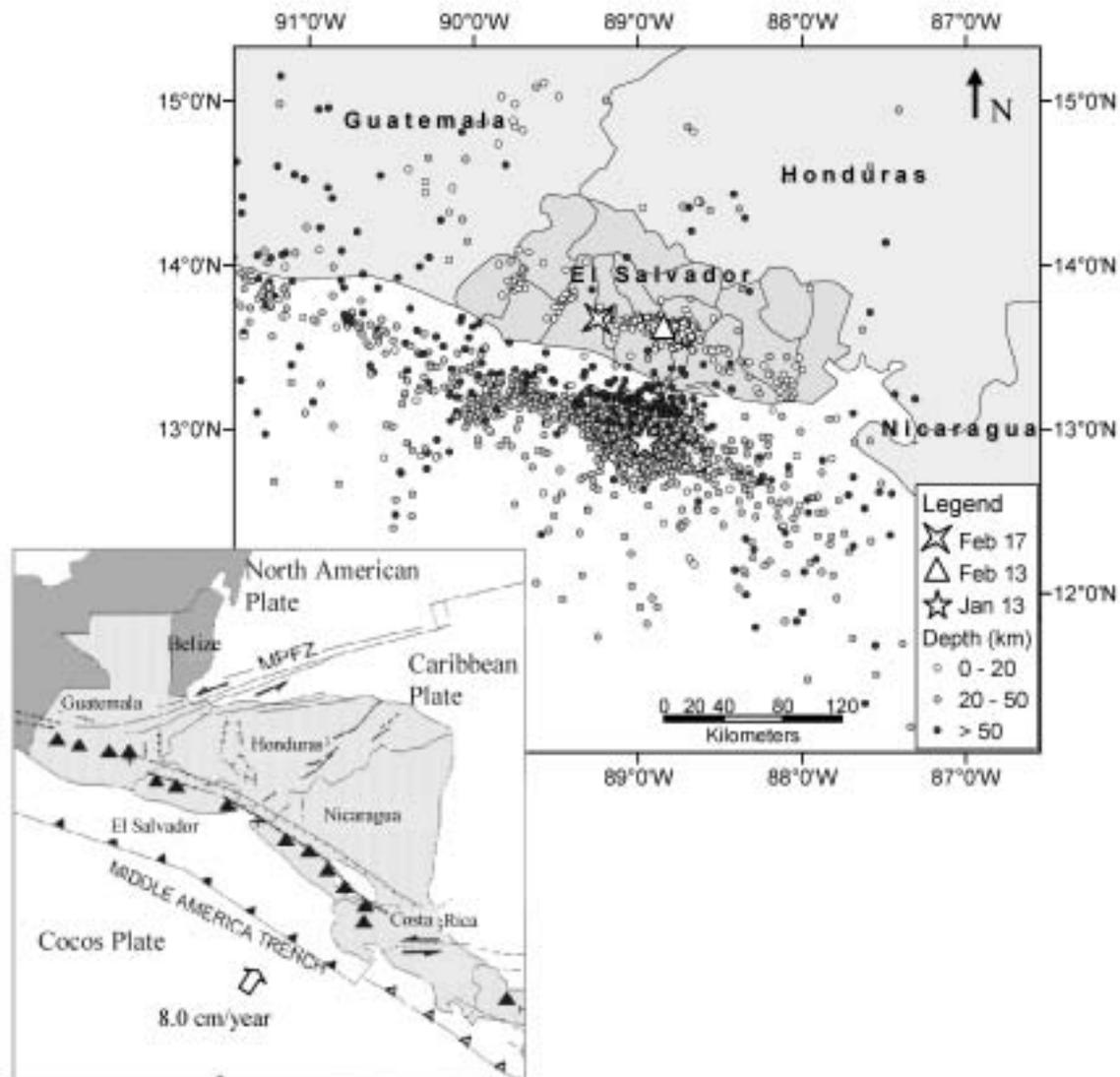
Figure 1. Map showing the distribution of seismicity during 2001, recorded and relocated by the Salvadoran Short-Period Network of the Center for Geotechnical Investigations (CIG). Estimation of the parameters was carried out with SEISAN system (Earthquake Analysis Software, 2000). Inset shows Regional Tectonics of Central America (after Rojas et al., 1993). Solid and open triangles indicate thrust faulting at subduction and collision zones, respectively. Large open arrows are plate motion vectors; half arrows indicate sense of movement across strike-slip faults, ticks indicate downthrown side of normal faults. Large solid triangles are Quaternary volcanoes. MPFZ—Motagua-Polochic fracture zone.

The two large shocks of 13 January and 13 February, together with events of lesser magnitude and their respective aftershock sequences, produced an intense period of seismic activity during a short time interval. This activity at a certain moment did not appear to decrease in time and frequency, according to the laws known. The study of the spatial and time distribution of these series, related to the tectonic environment and the stress transfer evolution, is the main purpose of this paper. The historical seismicity in El Salvador shows that large subduction events are commonly followed by crustal earthquakes in a time interval of four to five years (White, 1991). The main question we address here is whether the M 6.6 February 13 earthquake was in some way triggered by the larger subduction earthquake a month earlier. This behavior would be important for future seismic hazard in the area.

SEISMOTECTONIC ENVIRONMENT

The seismic activity registered in 2001 is framed in the particular seismotectonic context of El Salvador, and of Central America at a regional scale, which has been already described by many authors (Dewey and Suarez, 1991; Ambraseys and Adams, 2001; White and Harlow, 1993; Bommer et al., 2002).

The El Salvador earthquakes of 2001 are associated with the two principal seismic sources that define the seismotectonic structure of Pacific Central America. The largest earthquakes are generated in the subducted Cocos plate and its interface with the Caribbean plate beneath the Middle America trench (Dewey and Suarez, 1991). Relative plate motion of 8 cm/yr produces frequent earthquakes extending to intermediate depths (~200 km), beneath the Pacific Coast of El Salvador. Some earthquakes in this zone in the past century include those of 7 September 1915 (M_S = 7.7), 28 March 1921 (M_S = 7.4), 21 May 1932 (M_S = 7.1), and 19 June 1982 (M = 7.3) (Ambraseys and Adams, 2001).

A second major source of seismicity is related to a local system of faults that extends from west to east along the volcanic chain. These upper-crustal earthquakes have a tectonic origin, but are often called "volcanic chain events" due to their proximity to the volcanic axis. The majority of the events in this source have moderate magnitudes (5.5 < M < 6.8) and shallow depths (h < 20 km). These events contribute significantly to the seismic hazard and risk in the region, and historically have caused more deaths and damage than large earthquakes in the subduction zone (White and Harlow, 1993). During the twentieth century such earthquakes struck El Salvador on at least seven occasions, sometimes occurring in clusters of two or three similar events with a time difference of minutes or hours (White and Harlow, 1993) (Table 1 and Fig. 2).

The 2001 earthquakes of 13 January and 13 February are recent examples of the seismic potential of the subduction zone and the volcanic chain. Specifically, the event of 13 January is similar to that of 19 June 1982 in terms of mechanism, focal depth, and of the damage pattern in the southwest of the country. This earthquake was followed by the crustal event in 1986. On the other hand, the location of the 13 February event is similar to that which occurred in 1936, which was preceded by the subduction event in 1932.

Regarding the focal mechanism for both types of earthquakes, different authors give solutions for the subduction events of 1982 and of 13 January 2001, corresponding to normal faulting with horizontal extension in NE-SW direction. The shallow crustal events in 1965, 1986, and February 2001 present a strike-slip mechanism, with vertical fault planes oriented in NS and EW directions.

A tectonic interpretation of the region given by Harlow and White (1985) suggested that the relative motion between the Caribbean and Cocos plates is slightly oblique and decoupled into two components: a larger normal component, manifest as thrust faulting along the Middle America trench; and another smaller

TABLE 1. SOURCE PARAMETERS OF THE DESTRUCTIVE EARTHQUAKES IN EL SALVADOR
THROUGHOUT THE TWENTIETH CENTURY

Year	Month	Day	Hour	Latitude (°)	Longitude (°)	MS	Depth (km)	Intensity (MM)	Source
1915	09	07	01:20	13.90	−89.60	7.7	60	IX	Subduction
1917	06	08	00:51	13.82	−89.31	6.7	10	VIII	Local
1917	06	08	01:30	13.77	−89.50	5.4	10	VIII	Local
1919	04	28	06:45	13.69	−89.19	5.9	10	X	Local
1930	07	14	22:40	14.12	−90.25	6.9	30	VII	Local
1932	05	21	10:12	12.80	−88.00	7.1	150	VIII	Subduction
1936	12	20	02:45	13.72	−88.93	6.1	10	VIII	Local
1937	12	27	00:43	13.93	−89.78	5.9	10	VII–VIII	Local
1951	05	06	23:03	13.52	−88.40	5.9	10	VIII	Local
1965	05	03	10:01	13.70	−89.17	6.3	15	VIII	Local
1982	06	19	06:21	13.30	−89.40	7.3	80	VII	Subduction
1986	10	10	17:49	13.67	−89.18	5.4	10	VIII–IX	Local
2001	11	03	17:33	13.05	−88.66	7.8	60	VIII	Subduction
2001	02	13	14:22	13.67	−88.94	6.5	10	VIII	Local

4   *B. Benito, J.M. Cepeda, and J.J. Martinez Diaz*
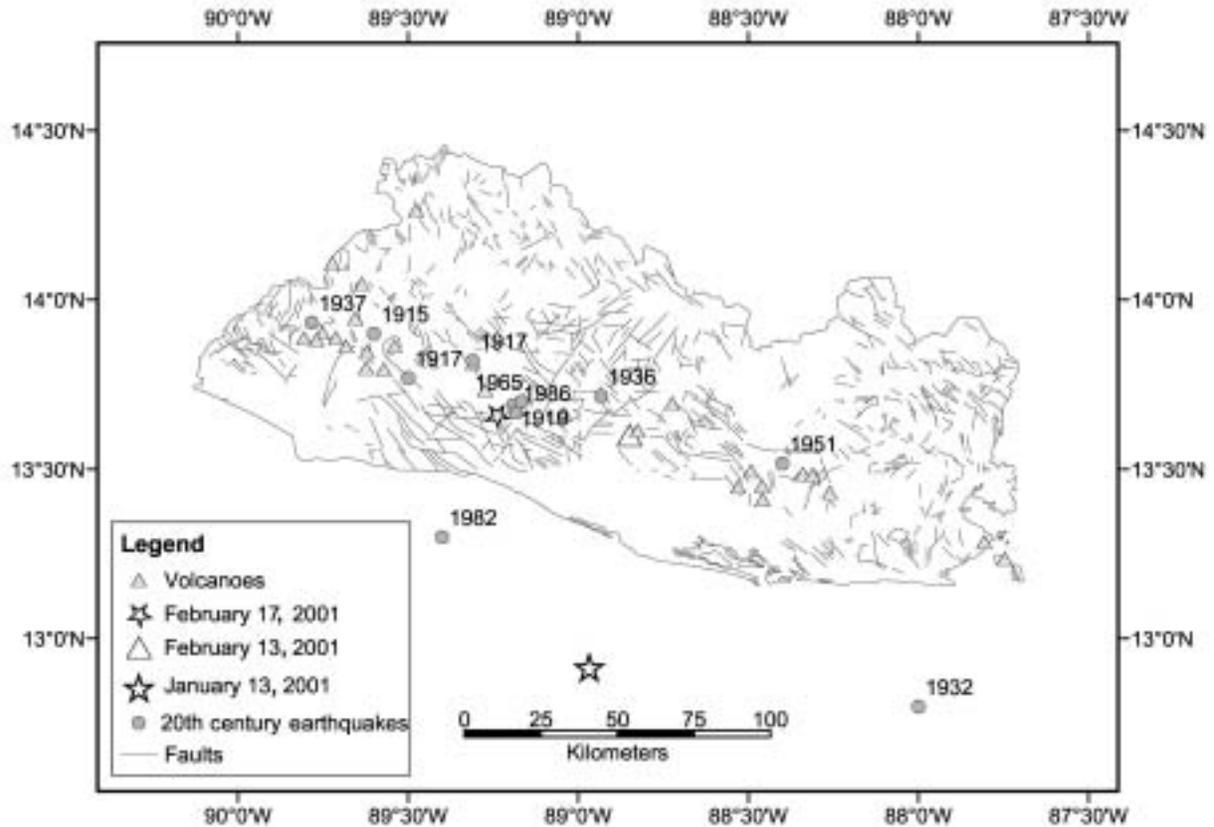
Figure 2. Local tectonic map of El Salvador with locations of the main shocks of the twentieth century (epicenters represented by circles) and the beginning of 2001 (special symbols) and the active volcanoes (triangles). A list with the parameters of these earthquakes is included in Table 1.

longitudinal component, manifest as right-lateral shear along the volcanic chain. The focal mechanisms and geologic features along the volcanic zone are compatible with the interpretation of this zone as a strike-slip right-lateral shear zone caused by an oblique component of Cocos-Caribbean collision (White, 1991). The existence of right-lateral slip faults within the volcanic arc of El Salvador and adjacent regions of Guatemala and Nicaragua (Weinberg, 1992), and the clustering of earthquakes along these faults, is consistent with the trench-parallel component of motion concentrated along the volcanic chain (DeMets, 2001). The rate of the strike-slip motion along the arc is estimated to be 8 mm/ yr (Guzman-Speciale, 2001), the motion being parallel to the trench. In both El Salvador and Guatemala this rate is predicted to be slower than in Nicaragua, due to the extension east of the forearc (DeMets, 2001). Recent geodetic observations in the region not only support the model of strain partitioning proposed by Harlow and White (1985) but also constrain the rate of forearc slip (DeMets, 2001).

In this tectonic environment, normal-faulting subduction earthquakes are usually followed within four or five years by large thrust events or by shallow intraplate earthquakes. This behavior has been observed in other regions where the tectonic

regime involves subduction limit offshore and volcanic axis inside the continent, such as Mexico (Lomnitz and Rodríguez, 2001). This inference may be explained because the stress transfer due to relaxation in one area leads to heightened tectonic stress in adjacent areas. The present study shows that a similar pattern may exist in El Salvador.

SPATIAL AND TEMPORAL CHARACTER OF THE 13 JANUARY AND 13 FEBRUARY 2001 EARTHQUAKES SEQUENCE

We focus on the 13 January and 13 February 2001 events, which were the largest shocks of that year, and on their respective aftershock series. Our study is intended to shed light on a possible interaction between both types of events.

Correlation between Magnitude Scales

The study aims to characterize the evolution of the seismicity recorded in El Salvador during 2001, taking into account the magnitude of the earthquakes that followed subsequently. For this purpose, a homogeneous magnitude is required, so we have calculated moment magnitude (M_w) for all the significant events included in the available catalog.

The El Salvador seismic catalog for 2001 compiled by the Servicio Nacional de Estudios Territoriales (SNET) contains 3755 events with magnitudes ranging from 2.1 to 7.8. The magnitude scales used are coda magnitude (M_C), local magnitude (M_L), surface wave magnitude (M_S), and moment magnitude (M_W).

Analyses of earthquake recurrence and strong-motion attenuation use magnitude in terms of M_S or M_W, to avoid saturation of local magnitude scales, such as M_C and M_L, for earthquakes larger than about M 7. In order to allow for comparisons of our analyses with other studies, a regression of the data was performed to obtain an M_W-M_C conversion relationship (Rojas et al., 1993).

A subset was created from the catalog, selecting events containing both magnitude scales. The subset was fitted to a second degree polynomial, which produced the best solution compared to the linear, logarithmic, power, and exponential forms. The resulting relation is given by:

$$M_w = -0.0155M_c^2 + 0.9731M_c + 0.3719 \qquad (1)$$

The correlation coefficient is 0.9. Figure 3 shows a plot of the M_W-M_C distribution from which the moment magnitude M_W has been estimated for all the events in the catalog.

Source Parameters

The source parameters of the studied shocks together with the focal mechanism, given by different agencies and authors, are shown in Tables 2A and 2B.

The source time function for the 13 January event indicates two subevents: the first with higher amplitude and 22 seconds duration, and a second one of 24 seconds (Bommer et al., 2002). The seismic moment release is 5.54×10^{20} Nm with no apparent directivity effects. The earthquake with intermediate depth occurred inside the down-going Cocos plate, its mechanism being a normal fault with subvertical fault plane and a tension (T-axis) subparallel to the dip direction of the descending slab.

For the 13 February event, located in the upper plate at the volcanic chain, the fault plane solution is a strike-slip event. This event occurred at a depth of 14 km, with a seismic moment of 6.05×10^{18} Nm and a total duration of 12 s (Bommer et al., 2002). The aftershock distribution delineates a rupture plane subparallel to the volcanic chain and thus subparallel to the trench.

Spatial Distribution of Aftershocks

The map depicted in Figure 1 shows the total distribution of events in 2001, relocated by the SNET. In that figure, it is possible to observe some clusters corresponding to the aftershock sequences of the different main shocks, with the largest clusters located around the epicenters of 13 January and 13 February events. Our purpose is to identify the aftershocks associated with both events, as well as their rupture surfaces.

To obtain an overview of the seismicity pattern and associate events with each series, we examined the distribution of the aftershocks week by week within the time period January 13 to June 7, 2001. The results are included in Figures 4A and 4B.

During the first week following the January 13 earthquake, different clusters of local events occurred in the upper plate inland, together with one offshore cluster in the southwest part of the main-shock rupture. In the second week, from 21 to 28 January, overall activity decreased and in the third and fourth weeks ceased altogether beneath the volcanic chain. There is a quiescent period of 15 days before the M_W 6.6 volcanic chain event of 13 February, following which seismicity increased along a system of faults located parallel and perpendicular to the coast and included the M 5 event of 17 February. At the same time, the subduction activity increased again during the week from 13 to 20 February, as if it had been reactivated by the two volcanic chain events. Analysis of subsequent weeks suggests further changes in the seismicity rate following events with moderate magnitude: 28 February (M 5.6, subduction), 16 March (M 5.7, subduction), 10 April (M 4.9, volcanic chain), 8 and 9 May (series of three shocks, M 4.8, 4.6, and 4.6, volcanic chain). Activity began to
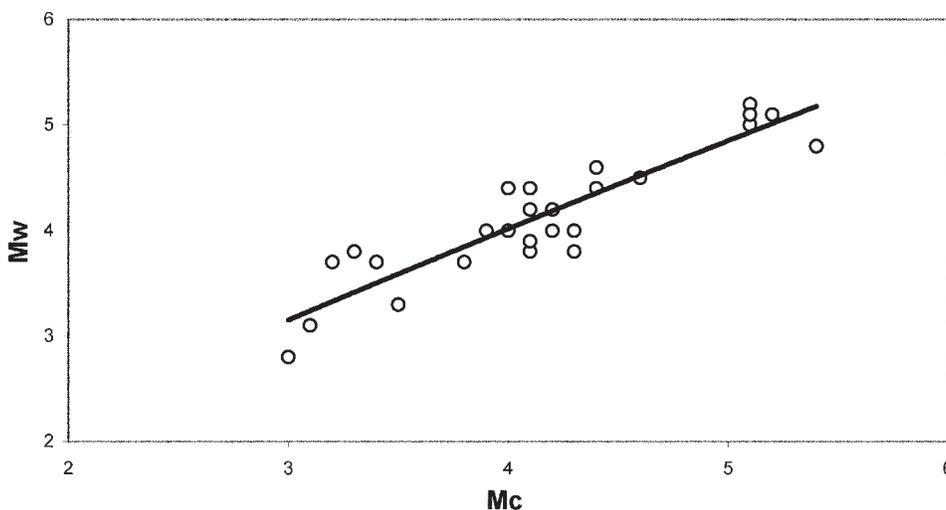
Figure 3. Relationship between coda and moment magnitude of events obtained from the subset used in the study. The agency source for magnitude is the Servicio Nacional de Estudios Terrotoriales (SNET), with the exception of the 13 January main shock, where the sources are the U.S. Geological Survey (USGS) and Central American Seismic Centre (CASC).

TABLE 2A. SOURCE PARAMETERS AND FOCAL MECHANISM FOR THE 2001 JANUARY 13 EVENT, ACCORDING TO DIFFERENT AGENCIES AND AUTHORS

Harvard (CMT)	USGS (CMT)	Buform et al., 2001 inversion P wave	CIG	CASC	Bommer et al., 2002
M_0: 4.6*10^{20} Nm	M_0: 2.9*10^{20} Nm	M_0: 5.54*10^{20} Nm	M_0:	M_0:	M_0: 5.54*10^{20} Nm
Mw: 7.7	Mw: 7.6	Mw: 7.8	Mw: 7.6	Mw: 7.7	Mw: 7.7
Time: 17:33:45.80	Time: 17:33:32.38	Time: 17:33:46	Local time: 11:34	Time: 17:33:30	
Epicentral location:	Epicentral location:	Epicentral location:	Epicentral location:	Epicentral location:	Epicentral location:
Lat 12.97° N	Lat 13.05° N	Lat 12.77° N	Lat 12.92° N	Lat 12.87° N	
Long 89.13°	Long. N 88.66° W	Long. 88.83° W	Long. 88.97° W	Long. 88.77° W	
Depth: 56 km	Depth: 36 km	Depth: 49 km	Depth: 32 km	Depth: 60 km	Depth: 50 km
		STF: 46 S			
			Localization: 45 km south, los Blancos Beach, Dpto. La Paz		2 sub-events of 22 and 24 s
p1: STK: 121°; DP: 35°; slip: –95°	p1: STK: 121°; DP: 37°; slip: –95°	p1: STK: 121°; DP: 35°; slip: –95°			
p2: 307°; 56°; –86°	p2: 307°; 54°; –86°	p2: ??			Fault plane: subvertical normal fault. Tension axis subparallel to dip direction of the descending slab.
		Rupture duration: 46 s			
Axis T, N Y P	Axis P, T Y N				
1. (T) VAL = 4.28; PL = 10; AZM = 35	1. (T) VAL = 3.17; PL = 9; AZM = 34	Complex rupture: most of released energy during the first 20 s.			
2. (N) –0.03; 3; 125	2. (N) –0.47; 3; 125				
3. (P) –4.55; 79; 231	3. (P) –2.70; 81; 233				

TABLE 2B. SOURCE PARAMETERS AND FOCAL MECHANISM FOR THE 2001 FEBRUARY 13 EVENT, ACCORDING TO DIFFERENT AGENCIES AND AUTHORS

Harvard (CMT)	USGS (CMT)	Buform et al., 2001 inversion P wave	CIG	CASC	Bommer et al., 2002
M_0: 8.1*10^{18} Nm	M_0: 6.2*10^{18} Nm	M_0: 6.05*10^{18} Nm	M_0:	M_0:	M_0: 6.05*10^{18} Nm
Mw: 6.6	Mw: 6.5	Mw: 6.5	Mw: 6.6	Mw: 6.6 (mc = 6.7)	Mw:
Time: 14:22:16.40	Time: 14:22:05.82	Time: 14:22:16	Local time: 08:22	Time: 14:22:09.80	Time:
Epicentral location:	Epicentral location:	Epicentral location:	Epicentral location:	Epicentral location:	Epicentral location:
Lat 13.98° N	Lat 13.67° N	Lat 13.60° N	Lat 13.60° N	Lat 13.44° N	
Long 88.97° W	Long. N 88.94° W	Long. 88.96° W	Long. 88.85° W	Long. 88.94° W	
Depth: 15 km	Depth: 15 km	Depth: 14 km	Depth: 8 km	Depth: 13.9 km	Depth: 14 km
		STF: 14 S			Duration: 12 s
p1: STK: 276°; DP: 74°; slip: –175°	p1: STK: 96°; DP: 81°; slip: –178°	p1: STK: 90°; DP: 191°; slip: –180°	Localization: San Pedro Nonualco. Dpto. La Paz.		Strike-slip. Fault plate subparallel to the subduction trench.
p2: 7°; 86°; –16°	p2: 6°; 88°; –9°	p2: 90°; 101°			
Axis T, N Y P	Axis P, T Y N				
1. (T) VAL = 8.50; PL = 14; AZM = 233	1. (T) VAL = 6.17; PL = 5; AZM = 51				
2. (N) –0.83; 73; 22	2. (N) –0.02; 81; 173				
3. (P) –7.66; 8; 141	3. (P) –6.14; 7; 321				

Figure 4 (*on this and following page*). A: Seismicity of El Salvador after the main shock of January 13 (white star) until March 28, for intervals of one-week duration (magnitude $M_w \geq 3.0$). The epicenter of the February 13 event is also represented after its occurrence (black star). The other events identified as changing the seismicity rates are also represented in their corresponding time windows (M 5.6, 28 February, subduction; M 5.7, 16 March, subduction). The locations of the remaining events are represented by circles, whose color shows the range of depths (white—h < 20 km, gray—20 < h < 50 km, black—h > 50 km). Representation has been done using a geographic information system, Arc-Info 8.0. B: Seismicity for the period from March 29 until June 7, with the same representation criteria as in Figure 4A. New symbols of epicenters in some time windows correspond to events that act as triggers (M 4.9, 10 April, volcanic chain; M 4.6, 10 April, subduction; and M 4.6, May 8 and 9, volcanic chain).
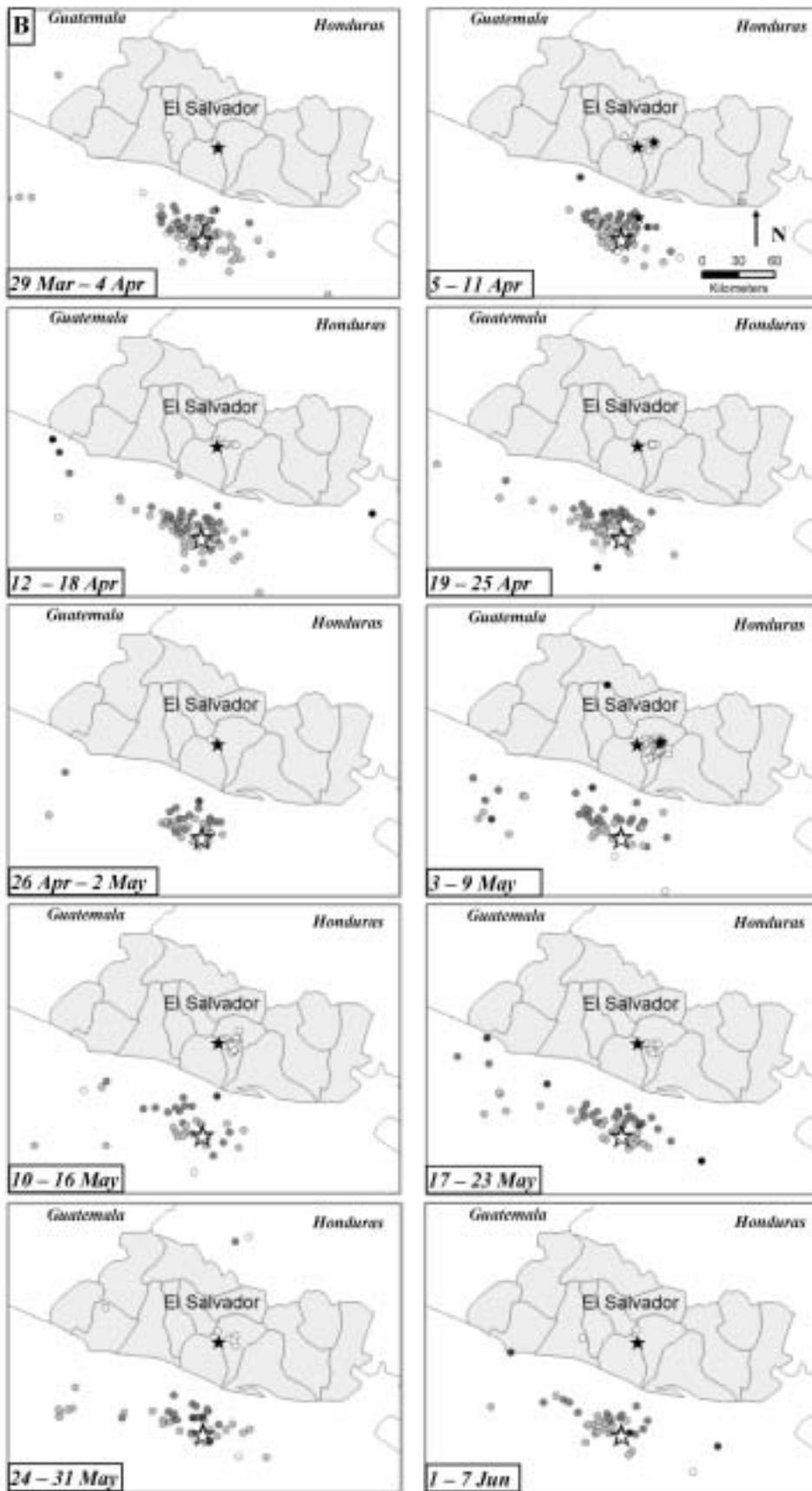
Figure 4 (*continued*).

subside in July, even though seven more events of M > 4.5 took place until the end of the year in both scenarios.

To sum up, the seismic activity as far as the subduction and the local strike-slip faults are concerned are alternately increasing and decreasing, with some weeks in which both types of seismicity seem to alternate. This tendency becomes evident as, coincidentally to the occurrence of new shocks with magnitude close to 5.0, the activity around their epicenters is again triggered. Therefore, such events can act as triggers of new shocks, inducing in turn other events with similar magnitude and different source. Due to the importance of these events in the global activity registered, which may be at the same time the cause and effect of itself, it is worthwhile to analyze them in detail. Table 3 shows the parameters of all the events registered during 2001 with magnitude M ≥ 4.5.

In summary, the temporal superposition of these series produced an unusual activity during the six first months of 2001. It appears that the 13 January earthquake triggered one or several local faults of the volcanic chain, and these in turn affected seismicity in the subduction area. One must consider whether the local events would have occurred in the absence of the 13 January earthquake. A reasonable supposition is that they would occur but perhaps not until much later. The historical seismicity of El Salvador shows that approximately every 20 yr a destructive volcanic earthquake occurs, and the last one took place in 1986 (White and Harlow, 1993). It is probable then that the fault on which the 13 February earthquake was originated had accumulated sufficient strain so that, although it might have not been released by itself at that time, the additional loading caused by the event of 13 January could have acted as a trigger.

Modeling of Rupture Surfaces

After studying the spatial distribution of the aftershock sequences, we now attempt to model the rupture planes associated with the earthquakes on 13 January and 13 February, starting with the distribution of the aftershocks for the first three days following the main shocks. In theory, the distribution for each aftershock series must define a plane obtained by the fit of the hypocenters, which agrees with the solutions given by the focal mechanism. However, when examining the solutions given by different agencies (Tables 2A and 2B), we can see that there are some differences among the values of azimuth and dip. Therefore, we intend to obtain more information from the aftershock areas, which allows us to confirm some of these solutions.

We have tested different orientations of faulting, centered in the aftershock cloud, according to the focal mechanism given in Tables 2A and 2B. Then we have looked for the best solution, as that which represents higher coherence between the mechanism and aftershock distribution.

For the January 13 event, our best-fit solution is a fault plane dipping 60° to the NE with a strike of N 128° E, subparallel to the Middle America trench (Fig. 5A). The fault has a length of 67 km and a rupture area of 2532 km², indicated by the spatial distribution of the aftershocks.

For the crustal earthquake of 13 February, the best solution indicates a plane of 471 km² striking N 94° E and dipping 70° SW (Fig. 5B).

Temporal Distribution of Aftershocks

We studied the temporal evolution of each aftershock sequence independently for the 13 January and 13 February events to assess the possible interaction between both series. In the second sequence, the foreshocks have also been included in the analysis. The discrimination of shocks associated with each series was made by taking the events associated with each surface rupture previously determined but extending the time interval through 2001. Figure 6 illustrates the number of events as a function of time for the two sequences and reveals alternating increases and decreases of activity in the respective source zones.

A significant feature is the occurrence of volcanic chain events from 13 to 25 January, which we interpret as local activity triggered by the previous subduction earthquake. The absence of local events during the following two weeks until February 13, when the main shock of this series took place, is also apparent.

These observations seem to corroborate the interaction between the sequences of different source, which can also be illustrated by superposing both series logarithmically with the same reference origin time (on 13 January), revealing strong irregularity for the two sequences (Fig. 7).

We also studied the decay of the aftershock activity analytically, with respect to Omori's Law (Omori, 1884), which in logarithmic form corresponds to the expression: $\log N(t) = a - b \log t$; $N(t)$ being the number of events by day and t the time in days from the main shock. Figure 8 shows the fit for each series in two time intervals. For the subduction sequence, a first fit is made for the whole series (six months) and a second fit taking only the events between 13 January and 13 February. The aftershocks can be seen to have decayed approximately according to Omori's law in the period up to 13 February, but they were gradually dying out when the second earthquake occurred (Fig. 8A). The fit is better if we only consider the aftershocks prior to the second major event (equation 3; Fig. 8B) rather than with the complete sequence (equation 2).

$$\log N(t) = 2.7 - 0.8 \log t, \text{ with } R^2 = 0.7 \qquad (2)$$

$$\log N(t) = 2.4 - 0.7 \log t, \text{ with } R^2 = 0.8 \qquad (3)$$

For the February 13 main shock and aftershock sequence an initial fit was made using the total set (Fig. 8C), in all the time interval, where it is possible to appreciate that the decreasing exponential rate is lost after 100 days approximately ($\log t = 2$), when the events of May 8 and 9 took place. A second test, considering only the events until this date (Fig. 8D), shows a better fit. The expressions derived for these two intervals are given respectively in equations 4 and 5:

TABLE 3. SUMMARY OF THE SOURCE PARAMETERS FOR THE EVENTS THAT OCCURRED IN 2001 WITH MAGNITUDE M ≥4.5

Year	Mo	Day	Hr	Min	Sec	Lat	Long	Depth (km)	Type	Magnitude	Agency
2001	1	13	17	35	52.7	12.92	−88.97	32.1	Subduction	$M_w = 7.6$	USGS
2001	1	16	8	23	24.3	13.33	−88.71	54	Subduction	$M_c = 4.6$	SAL
2001	1	16	10	59	32.2	13.04	−88.83	56.8	Subduction	$M_c = 4.9$	SAL
2001	1	16	11	25	48.0	13.00	−88.96	57.7	Subduction	$M_c = 4.5$	SAL
2001	1	17	1	36	18.7	12.93	−89.16	33.8	Subduction	$M_c = 4.6$	SAL
2001	1	17	21	5	40.5	12.93	−88.99	63.5	Subduction	$M_c = 4.6$	SAL
2001	1	25	10	28	51.8	12.79	−88.77	37.5	Subduction	$M_c = 4.8$	SAL
2001	2	2	8	10	43.7	12.89	−89.29	26.1	Subduction	$M_c = 5.1$	SAL
2001	2	7	10	23	11.3	13.03	−89.08	47	Subduction	$M_c = 5.1$	SAL
2001	2	13	2	50	57.0	12.00	−88.34	68	Subduction	$M_c = 4.5$	SAL
2001	2	13	14	22	05.8	13.60	−88.85	11.1	Volcanic chain	$M_w = 6.6$	SAL
2001	2	17	1	17	31.6	12.67	−88.96	50	Subduction	$M_c = 5.1$	SAL
2001	2	17	20	25	15.9	13.68	−89.25	5	Volcanic chain	$M_L = 5.1$	SAL
2001	2	21	6	51	28.1	12.98	−88.94	64.4	Subduction	$M_c = 4.7$	SAL
2001	2	23	18	40	56.8	13.04	−88.85	43.9	Subduction	$M_c = 4.5$	SAL
2001	2	24	3	46	52.1	13.49	−88.67	13.8	Volcanic chain	$M_c = 4.5$	SAL
2001	2	25	8	28	14.6	13.69	−89.23	8.5	Volcanic chain	$M_L = 4.6$	SAL
2001	2	26	19	51	10.2	12.64	−89.24	28.8	Subduction	$M_c = 4.7$	SAL
2001	2	28	18	50	14.5	13.00	−89.08	51.4	Subduction	$M_L = 5.6$	SAL
2001	3	16	0	1	19.6	12.84	−89.02	50	Subduction	$M_L = 5.7$	SAL
2001	3	18	15	43	23.1	12.58	−87.92	24	Subduction	$M_c = 5.2$	SAL
2001	3	29	6	54	31.6	13.04	−88.94	61.7	Subduction	$M_L = 5.4$	SAL
2001	4	3	1	7	14.2	12.83	−88.71	32.9	Subduction	$M_c = 4.5$	SAL
2001	4	10	3	16	53.9	13.08	−88.84	46.4	Subduction	$M_L = 4.9$	SAL
2001	4	10	21	46	58.9	13.64	−88.72	7.6	Volcanic chain	$M_c = 4.4$	SAL
2001	4	14	19	38	33.9	12.40	−88.74	17.9	Subduction	$M_c = 4.6$	SAL
2001	5	2	7	5	54.8	12.97	−89.09	40.4	Subduction	$M_c = 4.6$	SAL
2001	5	8	18	2	17.3	13.62	−88.71	9	Volcanic chain	$M_L = 4.8$	SAL
2001	5	8	18	15	47.0	13.61	−88.68	10.5	Volcanic chain	$M_L = 4.6$	SAL
2001	5	9	7	23	57.4	13.63	−88.67	18	Volcanic chain	$M_c = 4.6$	SAL
2001	6	2	19	36	36.4	12.83	−88.25	65.6	Subduction	$M_c = 4.7$	SAL
2001	6	6	19	27	46.9	12.27	−88.29	79.4	Subduction	$M_c = 4.5$	SAL
2001	7	17	20	1	52.3	12.62	−87.53	77.5	Subduction	$M_c = 4.8$	SAL
2001	9	6	22	59	53.5	12.34	−89.08	50	Subduction	$M_c = 4.5$	SAL
2001	9	18	14	50	58.2	13.04	−89.05	33.4	Subduction	$M_L = 5.0$	SAL
2001	11	9	0	49	37.9	13.32	−88.32	26.7	Subduction	$M_c = 4.6$	SAL
2001	12	1	9	0	04.9	12.72	−88.62	34.6	Subduction	$M_c = 4.6$	SAL

Note: USGS—United States Geological Survey; SAL—Salvadorian Local Network.
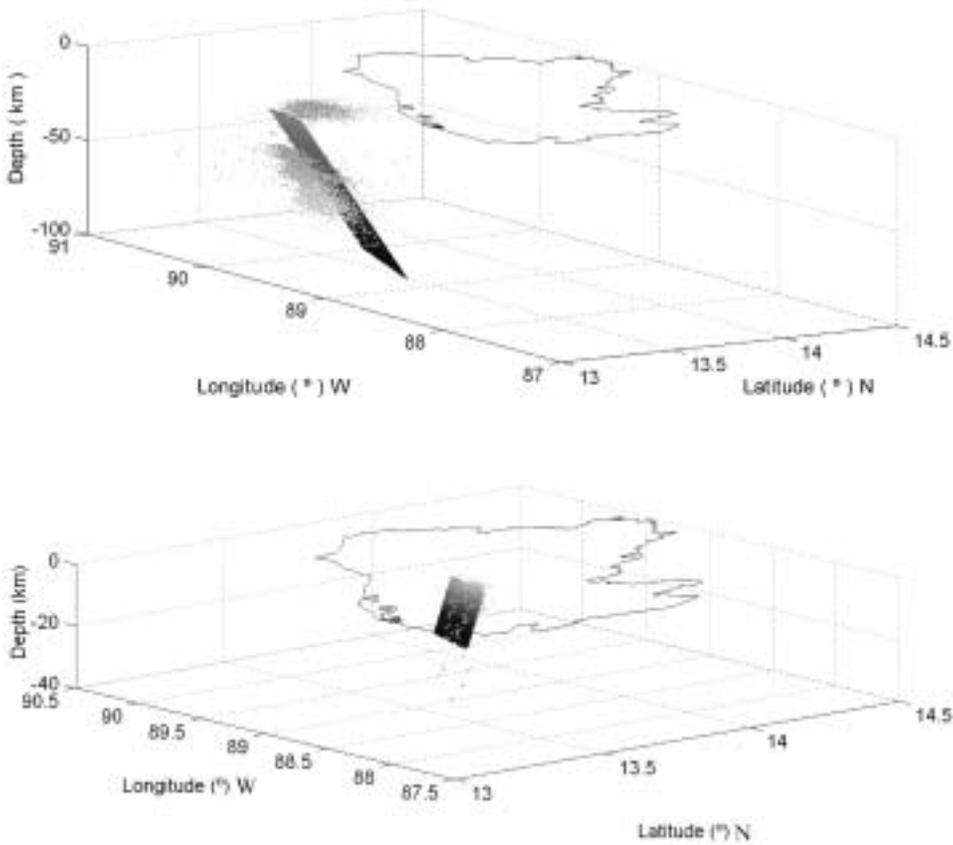
Figure 5. Fault plane of main shocks fitted to aftershocks of the first three days, together with the projection ellipse on the surface with the epicenters and the outline of El Salvador. A: Representation for the 13 January M_w 7.7 event. The fault trace is subparallel to the coast and the uppermost part of the rupture reaches a depth of 20 km. B: Representation for the 13 February M_w 6.6 event. The uppermost part of the rupture reaches a depth of 5 km, without breaking the surface, and most of the hypocenters are constrained to a depth less than 15 km.
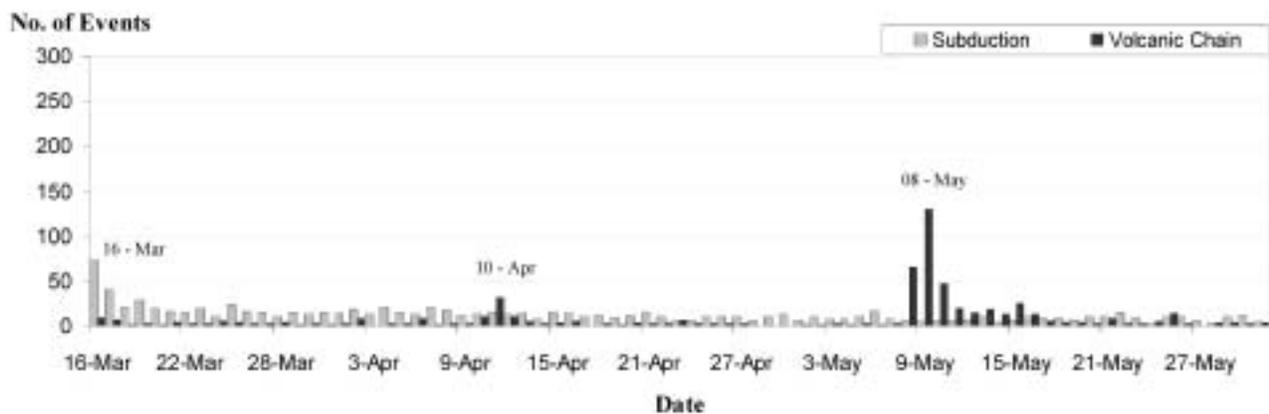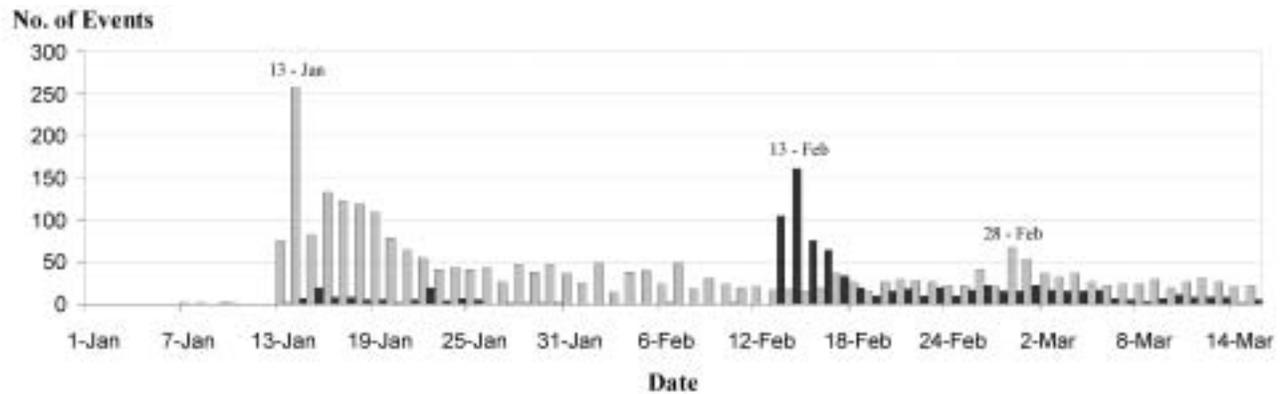
Figure 6. Histogram with the number of events as a function of time for the period January13–May 31, identifying with a different color those associated with 13 January and 13 February. It makes appreciable the occurrence of volcanic chain events from 13 January to 25 January, which can considered as local activity triggered by the previous subduction earthquake, and the total lack of local events during the following two weeks until February 13. Also remarkable is the alternating increase and decrease of subduction and volcanic chain events. The events that induce new activity are easily identified.
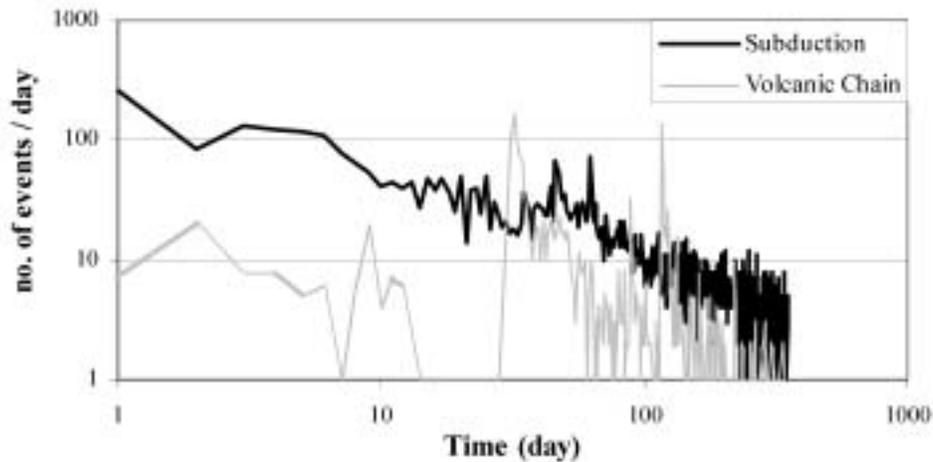
Figure 7. Joint temporal distribution of the aftershock series for January 13 and February 13, with reference to the origin time of the first main shock (13 January), in logarithmic scale. A strong irregularity for both series, in the temporal interval in which they are superposed, is observed.
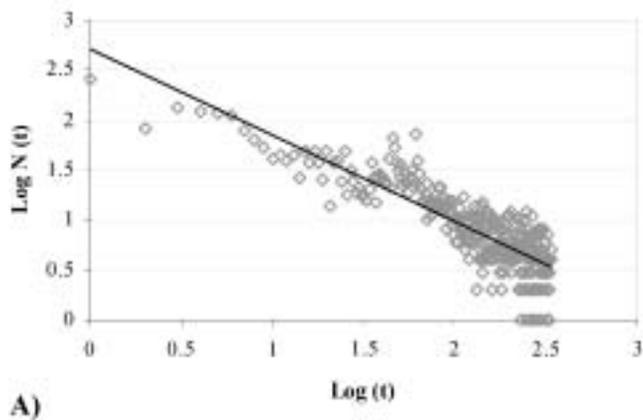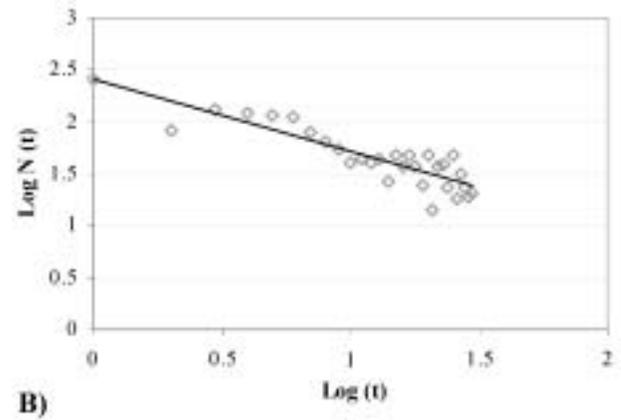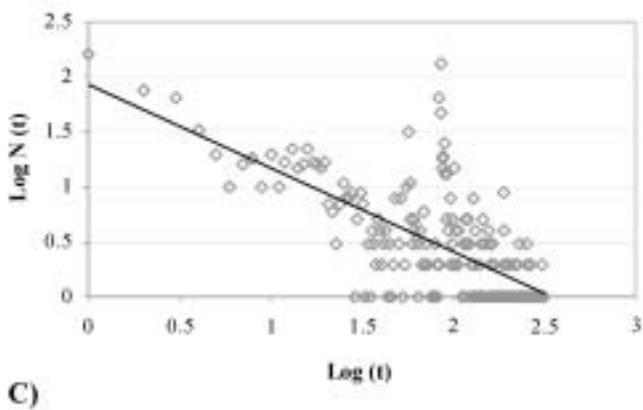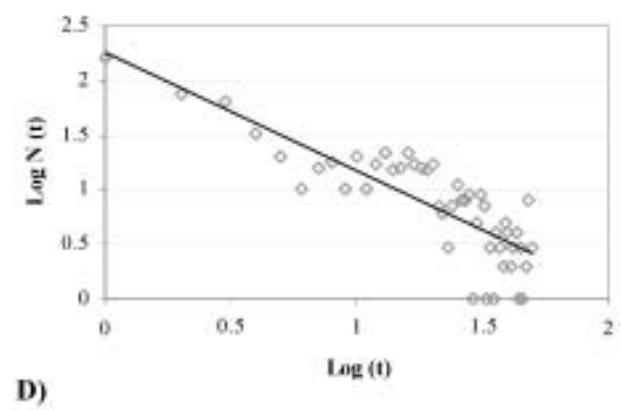
Figure 8. A: Fit to Omori's law for the total aftershock series of January 13 (six months). B: Fit to Omori's law only for the period between January 13 and February 13, prior to the second main shock. In this case the fitting is better than in the previous one. C: Fit to Omori's Law for the total aftershock series of February 13. D: Same as C for the period between February 13 and May 8, previous to the three local shocks with M > 4.6. A better fit is also found with regard to the total series.

$$\log N(t) = 1.9\text{–}0.7 \log t, \text{ with } R^2 = 0.5 \qquad (4)$$

$$\log N(t) = 2.3\text{–}1.1 \log t, \text{ with } R^2 = 0.7 \qquad (5)$$

The results confirm a perturbation to the lineal fit of after-shock decay when another earthquake with moderate magnitude occurred. A similar result was found in the analysis of the after-shock sequence of the M_W 7.6 August 17, 1999, Izmit, Turkey, earthquake. The time distribution of aftershocks follows Omori's law, except for the perturbations due to the activity following events of magnitude ~5, in particular the M 5 Marmara Island shock of September 20 (Polat et al., 2002).

Magnitude-Frequency-Depth Distribution of Aftershocks

The magnitude–frequency distribution of earthquakes commonly follows a power law of the Gutenberg-Richter form: log N(m) = a–bm; where "m" is a threshold magnitude and N(m) a cumulative number of earthquakes with M ≥ m. We computed parameters for the 13 January and 13 February series and obtained the equations 6 (subduction) and 7 (volcanic chain), as follows:

$$\log N(m) = 6.2\text{–}1.0 \, m, \text{ with } R^2 = 0.9 \qquad (6)$$

$$\log N(m) = 5.6\text{–}1.1 \, m, \text{ with } R^2 = 0.9 \qquad (7)$$

In both cases the parameter b was close to unity, with a high correlation ($R^2 = 0.9$). A lower value for parameter a was obtained for the volcanic chain events (13 February) and indicates less activity rate for the crustal events than for the subduction zone, as could be expected, given the source dimensions.

Finally, magnitude versus depth was also assessed for the two sequences of aftershocks (Fig. 9). The lesser magnitude and depth for the volcanic chain is clearly observed. The larger aftershocks (M > 5) of the subduction series are deeper than 25 km. The higher stress of rocks in deeper levels of the seismo-genic crust produce higher stress drops in deeper faults and may explain the observed difference in magnitude (Scholz, 1990).

MODELING OF STATIC COULOMB STRESS TRANSFER: TRIGGERING MECHANISM

The space-time relationship between the two main earth-quakes and their aftershock series invites the study of possible causal relations between both events resulting from dynamic and from static changes in the state of stress. Such changes may advance or retard the failure of faults in the region, as proposed in other seismically active regions, for instance the North Anatolian fault zone (Stein, 1999), and in particular the Marmara area after the Izmit earthquake (Parsons et al., 2000).

In the historical period, several large (M > 7) subduction earthquakes along the Cocos and Caribbean plate boundary have been succeeded by shallower crustal earthquakes in the volcanic chain in time intervals of years or months (White and Harlow, 1993; Bommer et al., 2002). This suggests the existence of a dynamic interaction between the faults of these principal seismic source zones. We have modeled the stress transfer produced by the main shocks on January 13 and February 13 using the param-eters of the rupture surfaces consistent with the regional tectonics and the seismological data.

It is known that the stress drop on a fault plane due to the occurrence of an earthquake produces an increase of effective shear stress around the rupture area (Chinnery, 1963). This trans-fer of the static stress may explain the generation and location of aftershocks and other main shocks at large distances from the fault, even at tens of kilometers, in those zones where the increase of the Coulomb failure stress (CFS) is ~1 bar. This fact has been recognized in numerous works in different geodynamic
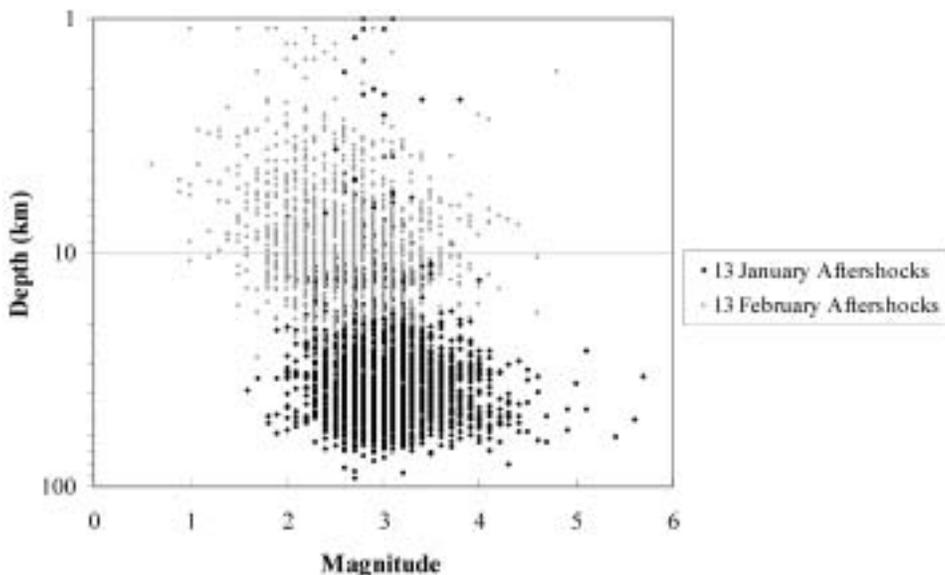
Figure 9. Magnitude versus depth for the two sequences of 13 January and 13 February. Most of the hypocenters of subduction events have depths in the range (20–80 km), while this range for local events is 3–20 km. The larger aftershocks (M > 5) of the subduction series have depths >25 km.

B. Benito, J.M. Cepeda, and J.J. Martinez Diaz

frameworks since 1992 (e.g., Jaumé and Sykes, 1992; King et al., 1994; Toda et al., 1998). The peculiarities of the El Salvador seismic sequences give special interest to this kind of analysis.

Methodology

During the last ten years, observations of seismicity from different seismogenic settings and magnitudes have indicated that variations in static stress less than 1 bar are able to induce the reactivation of nearby faults that are close to failure, either as aftershock activity or as larger earthquakes. This phenomenon has been described as a triggering process (King et al., 1994; Harris et al., 1995). It has also been observed that the triggering process may involve not only the generation of aftershocks or major shocks, but also changes of seismicity rate in a certain zone, increasing or decreasing for several months after a main shock (Stein and Lisowski, 1983; Reasenberg and Simpson, 1992; Stein, 1999).

The triggering effect is attributed to changes in Coulomb failure stress (CFS):

$$CFS = \tau_\beta - \mu\,(\sigma_\beta - p) \tag{8}$$

where τ_β is the shear stress over the fault plane, σ_β is the normal stress, p is the fluid pressure, and μ is the frictional coefficient.

For the seismic series of 2001 in El Salvador, we have estimated the change in the static Coulomb failure stress by the expression given in equation 9:

$$\Delta CFS = \Delta\tau_\beta - \mu'\,\Delta\sigma_\beta \tag{9}$$

where $\Delta\tau_\beta$ is considered positive in the direction of the slip fault, and $\Delta\sigma_\beta$ is also positive in a compressional regime. μ' is the apparent coefficient of friction and includes the effects of pore fluid as well as the material properties of the fault zone (see Harris, 1998, for a deeper explanation of this parameter). The positive values for ΔCFS are interpreted as promoting faulting, while negative values inhibit the activity.

We have estimated the stress change in an elastic half-space following the Okada (1992) method, taking for the shear modulus a value of 3.2×10^{10} N m^{-2} and for the Poisson coefficient a value of 0.25. The apparent friction coefficient is taken as 0.4, which is an acceptable value as proposed by Deng and Sykes (1997) from the study of 10 yr of seismicity in southern California. The introduction of different values for the apparent frictional coefficient, ranging from 0.2 to 0.6, does not produce significant changes in the obtained results.

Models of stress transfer have been constructed for the ruptures associated with the January 13 and February 13 earthquakes, respectively. The dimension and orientation of the surface ruptures are those derived earlier, taking into account the focal mechanisms published in previous studies.

The surface rupture estimated for the January earthquake (M 7.7) is ~2500 km^2. The focal mechanism calculated by Harvard

University, U.S. Geological Survey, Buforn et al. (2001), and Bommer et al. (2002) using different approaches (CMT [Centroid Moment Tensor] and wave polarities) (see Table 2A) gives practically the same orientation for the fault plane solution, between N 120° E and N 129° E. This direction agrees with the orientation of the horizontal axis of the ellipse fitted with the aftershock sequence. A bigger discrepancy is found for the dip of the fault, ranging from 48° NE to 63° NE. Taking into account the spatial distribution of the aftershocks, our model has been built for a plane oriented N 128° E dipping 60° NE, in agreement with the rupture solution presented earlier. The rake of the slip vector used is 98°, following the focal mechanism of Buforn et al. (2001), which corresponds with a normal fault. The aftershock sequence delineates a rupture extending between 15 and 78 km in depth.

In the case of the February event (M 6.6), the aftershock distribution, as well as the focal mechanism estimated by the U.S. Geological Survey and Buforn et al. (2001), indicate a steeply dipping, dextral strike-slip rupture plane, oriented N 94° E dipping 70° SW. The rupture area previously estimated from the aftershock distribution is 471 km^2. This result is consistent with the empirical magnitude/rupture area relationships of Wells and Coppersmith (1994).

Results and Interpretation

We obtained a model of Coulomb failure stress change for the January 13 event, which is included in Figure 10. Figure 10A represents a map view of the model for the January M 7.7 earthquake made for a horizontal plane at 14 km depth, which is the focal depth of the 13 February, M 6.6 earthquake. The color scale represents the different values in bars of the static Coulomb stress change generated by the rupture on planes parallel to the local fault reactivated on February 13 (N 94° E, 70° S). The epicenters of the main shock and the aftershocks produced 48 hours after the two main shocks are also projected. Figure 10B represents a cross section of the same model and shows that the February sequence occurs in an area where the January event produced an increase of CFS.

The stress change produced by the February 13 event is in general lower, but the shallower depth of the rupture produces strong effects in the surrounding area. Figure 11A shows a map view of the stress change produced by this strike-slip event across planes parallel to the January rupture plane, calculated for a 5 km depth horizontal plane (focal depth of the 17 February event). The February 17 event occurred on a lobe where CFS increased more than 0.8 bars following the February 13 event. We also observe that the aftershock area of the January event suffered either relative increase or decrease of CFS. Figure 11B represents the model of CFS change produced by the two main ruptures (M 7.7 and 6.6) on planes parallel to the February plane of rupture. After this event, significant areas of the volcanic chain are affected by increase of CFS higher than 0.4 bars. The aftershocks with magnitude higher than 4.5 of February 17, February 24, and November 11 occurred in areas of stress increase (Fig. 11B).
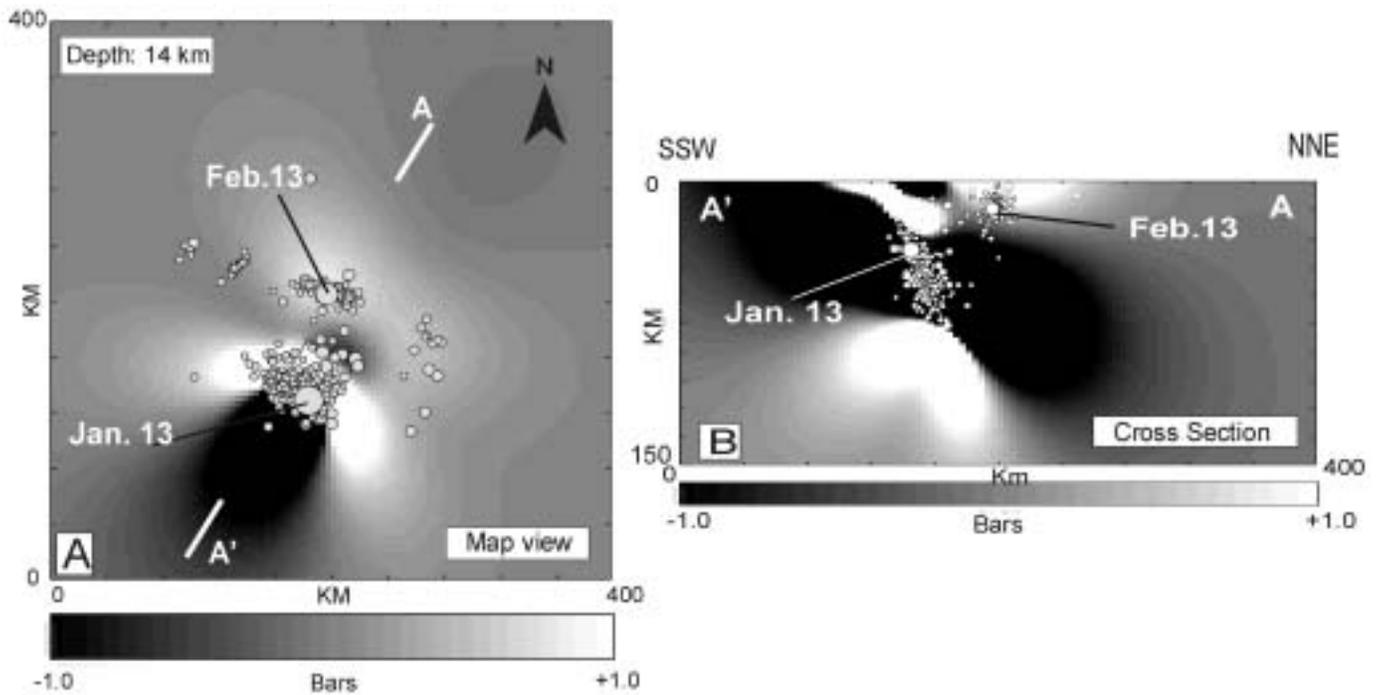
Figure 10. Inferred Coulomb stress transfer produced by the 13 January 2001 subduction earthquake. White and gray colors show the areas of predicted stress increase, while black represents the areas of predicted stress decrease. A: Map view for a horizontal plane, 14 km depth. B: NE-SW cross section view. The epicenters and hypocenters of the aftershocks that occurred within 48 hours of the two main shocks (13 January and 13 February) are shown. The location of the February sequence seems to be controlled by the lobe of increased stress produced by the January 13 event.
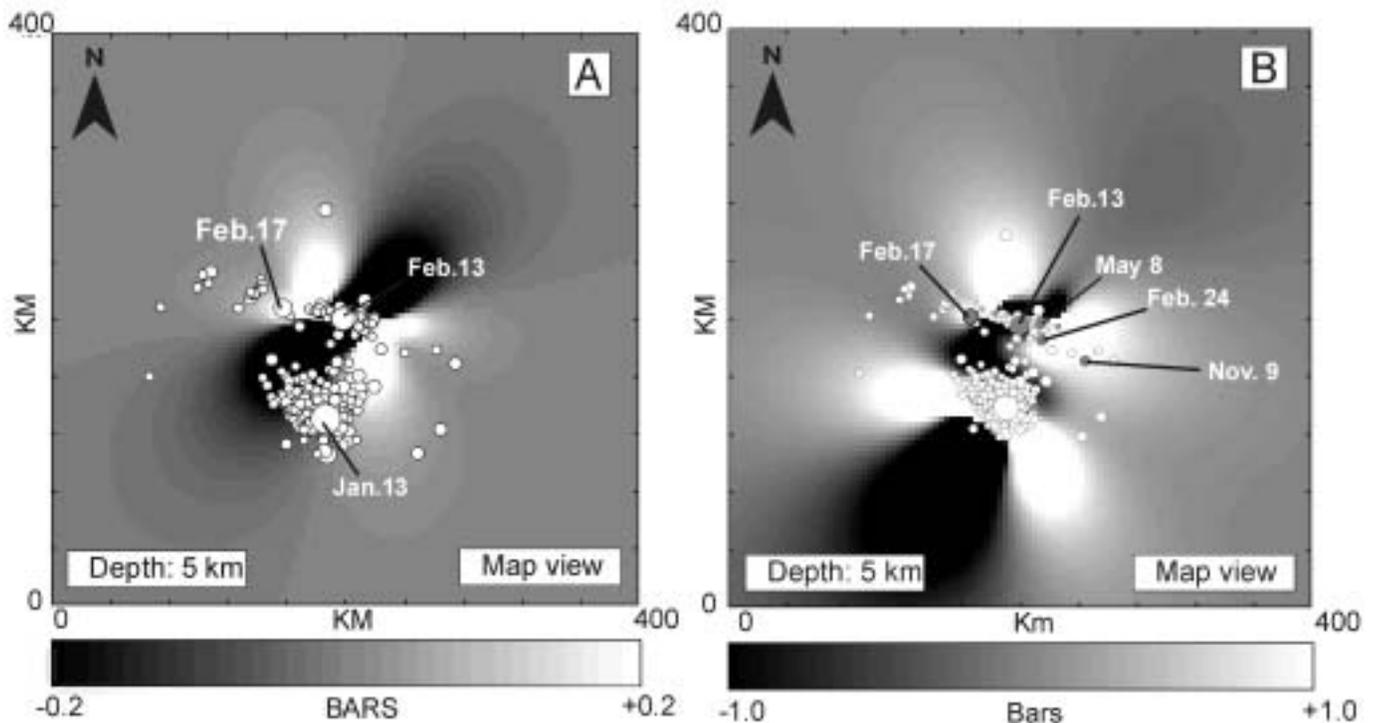
Figure 11. Coulomb stress transfer produced by the February 13, 2001, strike-slip earthquake. A: Model in map view for a horizontal plane at the focal depth of the 17 February event (5 km). This event occurred in a lobe of predicted stress increase. B: Stress transfer model for the two main shocks together in map view for a horizontal plane 5 km depth. The gray circles are the aftershocks of the volcanic chain with magnitude higher than 4.5, which occurred after the 13 February event.

However, the two aftershocks of May 8 happened in an area of reduced stress. Nevertheless, these two aftershocks are close to the rupture area of the February 13 event, where the development of static stress may be more complex.

In summary, we can conclude that the stress transfer generated by the January 13 event induced an increase of stress higher than 0.8 bars in the hypocentral zone of the February 13 event. Most of the aftershocks that occurred during the 48 hours after the February main shock are located in an area of increased CFS, and most of the aftershocks that delineate the rupture surface are located in the area with an increase higher than 1.5 bars. In turn, the February 13 shock increased the CFS by 0.4 bars in the hypocentral zone of the February 17 event (Fig. 11A).

On the other hand, the evolution of the aftershock rate for the January sequence seems to show a complex short-term dynamic evolution in the aftershock area. The change of CFS produced by the February 13 strike-slip event induced an increase of CFS up to 0.2 bars in the western part of the January rupture area and a decrease of CFS up to 0.18 bars in the eastern part. This process, repeated for all the local events with M > 4.5, may induce alternating stress increases and decreases either in time or in space, thus generating the observed complexity in the aftershock rate.

The correlation between CFS increases and observed seismicity in 2001, together with the historical pattern of subduction earthquakes followed by volcanic chain earthquakes, suggests that static stress transfer may be an important mechanism for this region. The events bigger than M 7 generated in the subducted Cocos plate are responsible for reactivating strike-slip faults along the volcanic chain on the Caribbean plate.

DISCUSSION

The study of the historical seismicity in El Salvador shows that large subduction earthquakes were often followed by shallow earthquakes along the volcanic chain in a time interval of 4 or 5 yr. The question we pose now is whether the 13 February 2001 earthquake was in some way triggered by the large subduction earthquake a month earlier.

One possible explanation is that the second event would have occurred anyway, without being triggered. A destructive volcanic chain earthquake has occurred in El Salvador approximately every 20 yr throughout the twentieth century, the last one in 1986. The 13 February event could simply have been the latest volcanic chain event in that series and thus could have occurred in the absence of the 13 January event.

However, the results of our study suggest that the 13 January earthquake triggered one or several local faults, and at the same time they were activated reciprocally and new events were induced in the area of the subduction event. The fault where the 13 February earthquake occurred probably had sufficient energy accumulated, and the stress storage derived from the adjustment of the tractions after 13 January acted as a trigger, in other words, "the straw that breaks the camel's back."

Anyway, many events in El Salvador have occurred in compound subduction–volcanic axis sequences throughout history. Of special interest should be the study of the time delay from the subduction to the continental events and also the study of the time interval between major subduction events. Figure 12 shows the time correlation between the main volcanic chain and subduction events from 1900 until 2001. Subduction events occur less frequently, that is, they have longer recurrence intervals than the volcanic chain events, but they also have larger magnitudes. A delay of three to four years for the continental events following the ones of subduction is also appreciated, with the exception of the two events of 2001. The analysis of these delays combined with the long-term stress loading derived from plate convergence can provide new insights into the mechanical coherence of a systematic triggering behavior.

CONCLUSIONS

A study of the spatial and temporal distribution of the earthquakes that occurred in El Salvador in 2001 has been carried out, with different purposes: first, to identify the aftershocks linked to each main shock; second, to model the corresponding rupture surfaces; and third, to know the evolution of the activity and the stress transfer associated with each rupture process. The results indicate that the M_w 7.7 event of 13 January in the subduction zone triggered later events associated with a system of crustal faults along the volcanic chain farther inland. The second destructive earthquake of M_w 6.6 on February 13 was located on one of these faults, near San Pedro de Nonualco. The superposition in such a short interval of time of both main shocks, together with the respective aftershock series, produced an intense period of activity that did not decay according to known laws, such as Omori's.

Our analysis of the ruptures and aftershock distribution leads us to the conclusion that the observed activity can be explained by interaction between the respective earthquakes' sources (subduction and local faults), whose aftershocks could have induced each other. Some events with a magnitude ~5 could be acting as triggers of other events with the same or different origin. Such events are, at the same time, the cause and the effect of the intense activity recorded.

On the other hand, the stress transfer after the two main shocks leads us to conclude that the 13 February event occurred in a zone where the Coulomb stress had increased by more than 0.8 bar following the January 13 event. A similar pattern may be inferred related to further events that occurred in the volcanic chain faults on February 17, due to the stress changes induced by the two previous shocks. The stress change also seems to have influenced the aftershock rate associated with the process.

Finally it is worth emphasizing the importance of the behavior of certain events as triggers of other events with a different origin in the seismic hazard of the region, and in other zones with a similar tectonic regime. A challenge for future study will be to model the conditions under which a subduction event may inter-
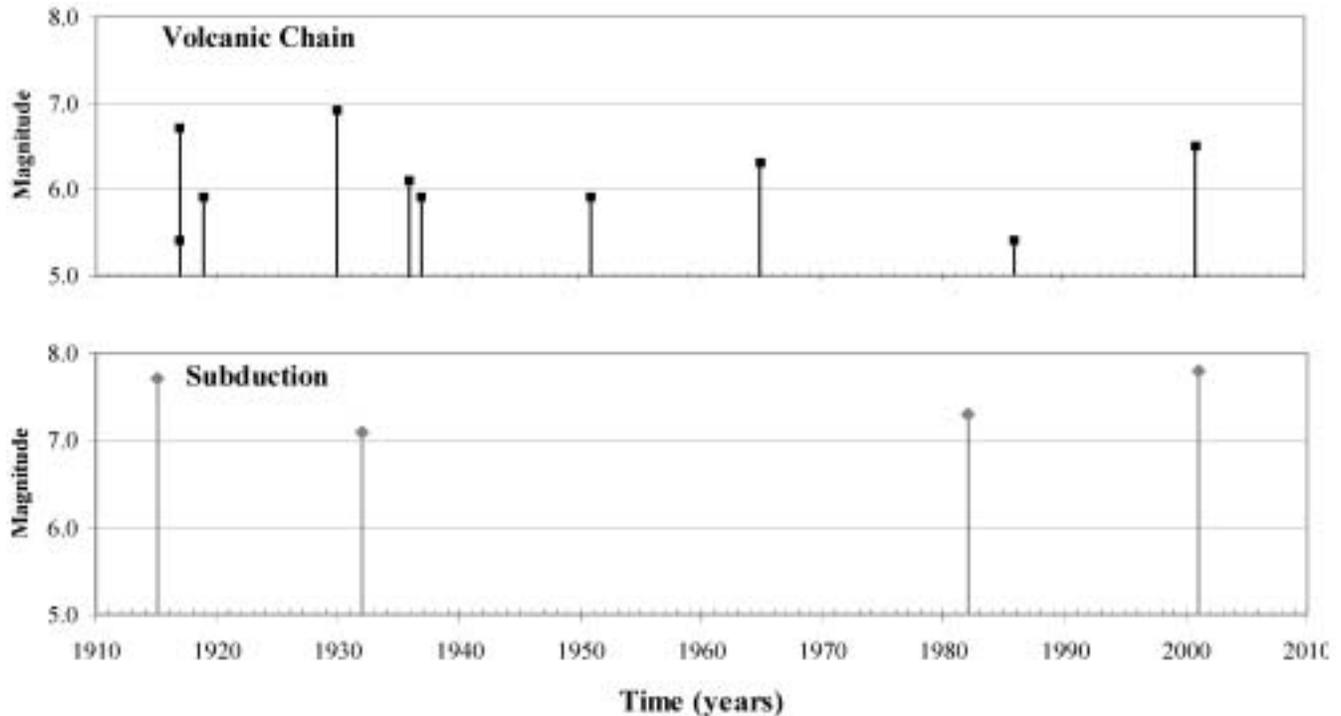
Figure 12. Temporal evolution of the main shocks in El Salvador from 1900 until 2001, showing magnitude versus time for volcanic chain events (top) and subduction events (bottom). The frequency of the last ones is lower and the magnitude higher than that for the local events. The delay of three to four years for the continental events following the ones of subduction is observed, with the exception of January 13 and February 13, 2001.

act with events of the volcanic chain, and to repeat processes such as the one studied in this paper. If the triggering mechanism can be modeled systematically, it may lead to improved estimates of earthquake recurrence and seismic hazard in El Salvador.

ACKNOWLEDGMENTS

REFERENCES CITED

Ambraseys, N.N., and Adams, R.D., 2001, The seismicity of Central America: A descriptive Catalogue1898–1995: London, Imperial College Press.

Bommer, J., Benito, B., Ciudad-Real, M., Lemoine, A., López-Menjivar, M., Madariaga, R., Mankelow, J., Mendez-Hasbun, P., Murphy, W., Nieto-Lovo, M., Rodríguez, C., and Rosa, H., 2002, The Salvador earthquakes of January and February 2001: Context, characteristics, and implications for seismic risk: Soil Dynamics and Earthquake Engineering, v. 22, no. 5, p. 389–418.

Buforn, E., Lemoine, A., Udias, A., and Madariaga, R., 2001, Mecanismo focal de los terremotos de El Salvador: 2º Congreso Iberoamericano de Ingeniería Sísmica, Octubre 2001, Madrid, p. 65–72.

Chinnery, M.A., 1963, The stress changes that accompany strike-slip faulting: Bulletin of the Seismological Society of America, v. 53, p. 921–932.

DeMets, C., 2001, A new estimate for present-day Cocos-Caribbean plate motion: Implications for slip along the Central American volcanic arc: Geophysical Research Letters, v. 28, no. 21, p. 4043–4046.

Deng, J., and Sykes, L.R., 1997, Stress evolution in southern California and triggering of moderate-, small-, and micro-sized earthquakes: Journal Geophysical Research, v. 102, no. 24, p. 411–435.

Dewey, J.W., and Suarez, G., 1991, Seismotectonics of Middle America, *in* Slemmons, D.B., et al., eds., Neotectonics of North America: Boulder Colorado, Geological Society of America, Decade Map, v. 1, p. 309–321.

Guzman-Speciale, M., 2001, Active seismic deformation in the grabens of northern Central America and its relationship to the relative motion of the North America–Caribbean plate boundary: Tectonophysics, v. 337, p. 39–51.

Harlow, D.H., and White, R.A., 1985, Shallow earthquakes along the volcanic chain in Central America: Evidence for oblique subduction: Earthquake notes, v. 55, p. 28.

B. Benito, J.M. Cepeda, and J.J. Martinez Diaz

Harris, R.A., 1998, Introduction to special section: Stress triggers, stress shadows, and implications for seismic hazard: Journal of Geophysical Research, v. 103, no. 24, p. 347–358.

Harris, R.A., Simpson, R.W., and Reasenberg, P.A., 1995, Influence of static stress changes on earthquake locations in southern California: Nature, v. 375, p. 221–224.

Jaumé, S.C., and Sykes, L.R., 1992, Change in the state of stress on the southern San Andreas fault resulting from the California earthquake of April to June 1992: Science, v. 258, p. 1325–1328.

King, G.C.P., Stein, R.S., and Lin, J., 1994, Static stress changes and the triggering of earthquakes: Bulletin of the Seismological Society of America, v. 84, p. 935–953.

Lomnitz, C., and Rodríguez, S., 2001, El Salvador 2001: Earthquake disaster and disaster preparedness in a tropical volcanic environment: Seismological Research Letters, v. 72, no. 3, p. 346–351.

Okada, Y., 1992, Internal deformation due to shear and tensile faults in a half space: Bulletin of the Seismological Society of America, v. 82, p. 1018–1040.

Omori, F., 1884, On the aftershocks of earthquakes: Journal College of Sciences, Imperial University, v. 7, p. 111–200.

Parsons, T., Toda, S., Stein, R., Barka, A., and Dieterich, J., 2000, Heightened odds of large earthquakes near Istanbul: An interaction based probability calculation: Science, v. 288, p. 661–665.

Polat, O., Eyidogan, H., Haessler, H., Cisternas, A., and Phillip, H., 2002, Analysis and interpretation of the aftershock sequence of the August 17, 1999, Izmit (Turkey) earthquake: Journal of Seismology, v. 6, p. 287–306.

Reasenberg, P., and Simpson, R., 1992, Response of regional seismicity to the static stress change produced by Loma Prieta Earthquake: Science, v. 255, p. 1687–1690.

Rojas, W., Bungum, H., and Lindholm, C.D., 1993, A catalogue of historical and recents earthquakes in Central America: Report NORSAR, 77 p.

Scholz, C., 1990, The mechanics of earthquakes and faulting: Cambridge, UK, Cambridge University Press, 439 p.

Earthquake Analysis Software, 2000, SEISAN for the IBM PC and SUN, Version 7.1, May 2000: Institute of Solid Earth Physics, University of Bergen, Norway.

Stein, R.S., 1999, The role of stress transfer in earthquake recurrence: Nature, v. 402, p. 605–609.

Stein, R.S., and Lisowski, M., 1983, The Homestead Valley earthquake sequence, California: Control of aftershocks and postseismic deformations: Journal Geophysical Research, v. 88, p. 6477–6490.

Toda, S., Stein, R.S., Reasenberg, P.A., and Dieterich, J.H., 1998, Stress transferred by the M_w = 6.5 Kobe, Japan, shock: Effect on aftershocks and future earthquake probabilities: Journal Geophysical Research, v. 103, no. 24, p. 543–565.

Weinberg, R.F., 1992, Neotectonic development of western Nicaragua: Tectonics, v. 11, p. 1010–1017.

Wells, D.L., and Coppersmith, K.J., 1994, New empirical relations among magnitude, rupture length, rupture width, rupture area and surface displacement: Bulletin of the Seismological Society of America, v. 85, no. 1, p. 1–16.

White, R., 1991, Tectonic implications of upper-crustal seismicity in Central America, *in* Slemmons, D.B., et al., eds., Neotectonics of North America: Boulder, Colorado, Geological Society of America, Decade Map, v. 1, p. 323–338.

White, R.A., and Harlow, D.H., 1993, Destructive upper-crustal earthquakes of Central America since 1900: Bulletin of the Seismological Society of America, v. 83, p. 1115–1142.